Supplement of Nonlin. Processes Geophys., 33, 267–302, 2026
https://doi.org/10.5194/npg-33-267-2026-supplement

Nonlinear Processes in Geophysics
Open Access
EGU

Supplement of

Structural joint modeling of magnetotelluric data and Rayleigh wave dispersion curves using Pareto-based particle swarm optimization: an example to delineate the crustal structure of the southeastern part of the Biga Peninsula in western Anatolia

Ersin Büyük et al.

Correspondence to: Ersin Büyük (ebuyuk@gumushane.edu.tr)

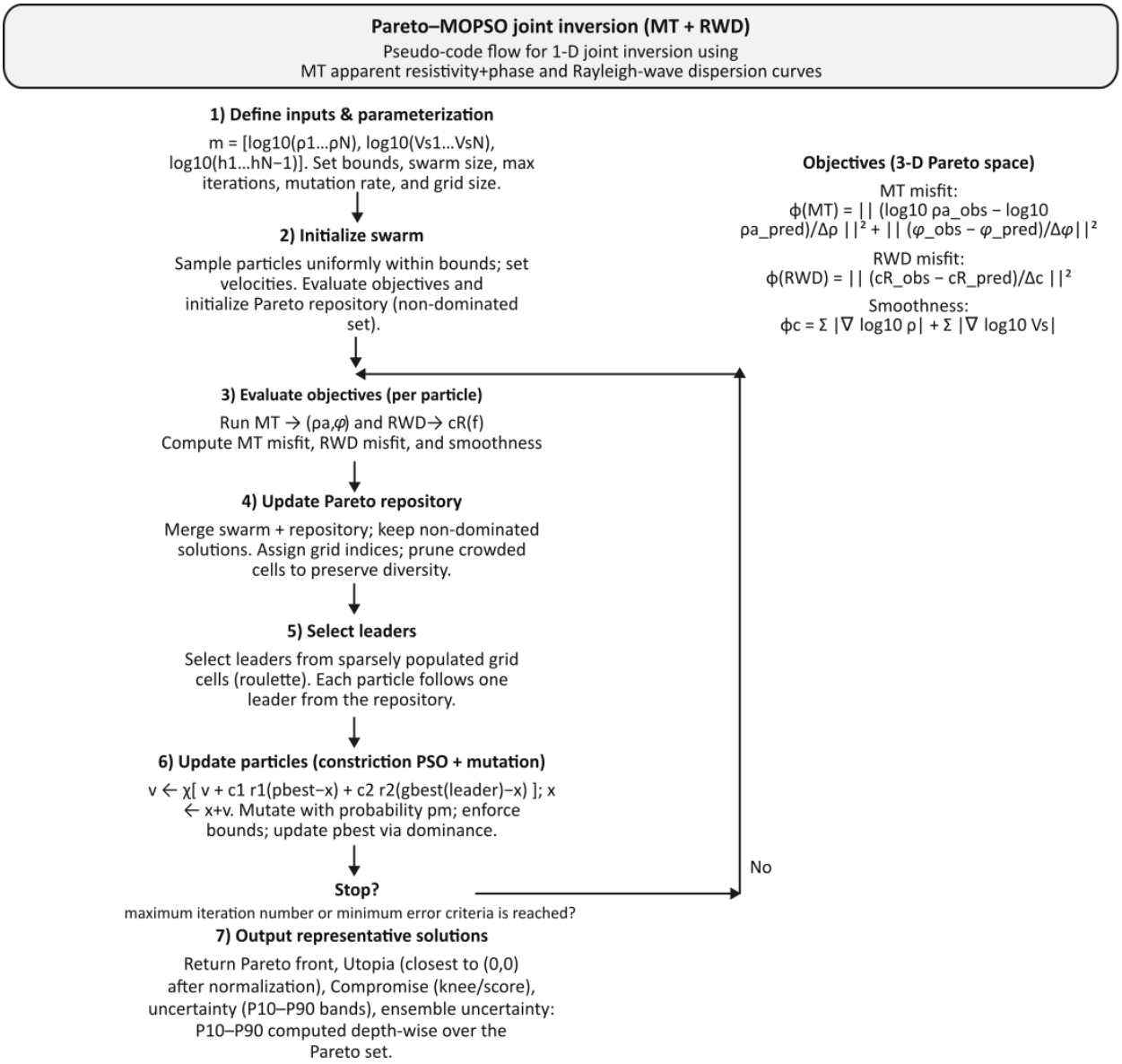

Figure S1. Flowchart (pseudo-code) of Pareto-MOPSO joint inversion (MT+RWD).

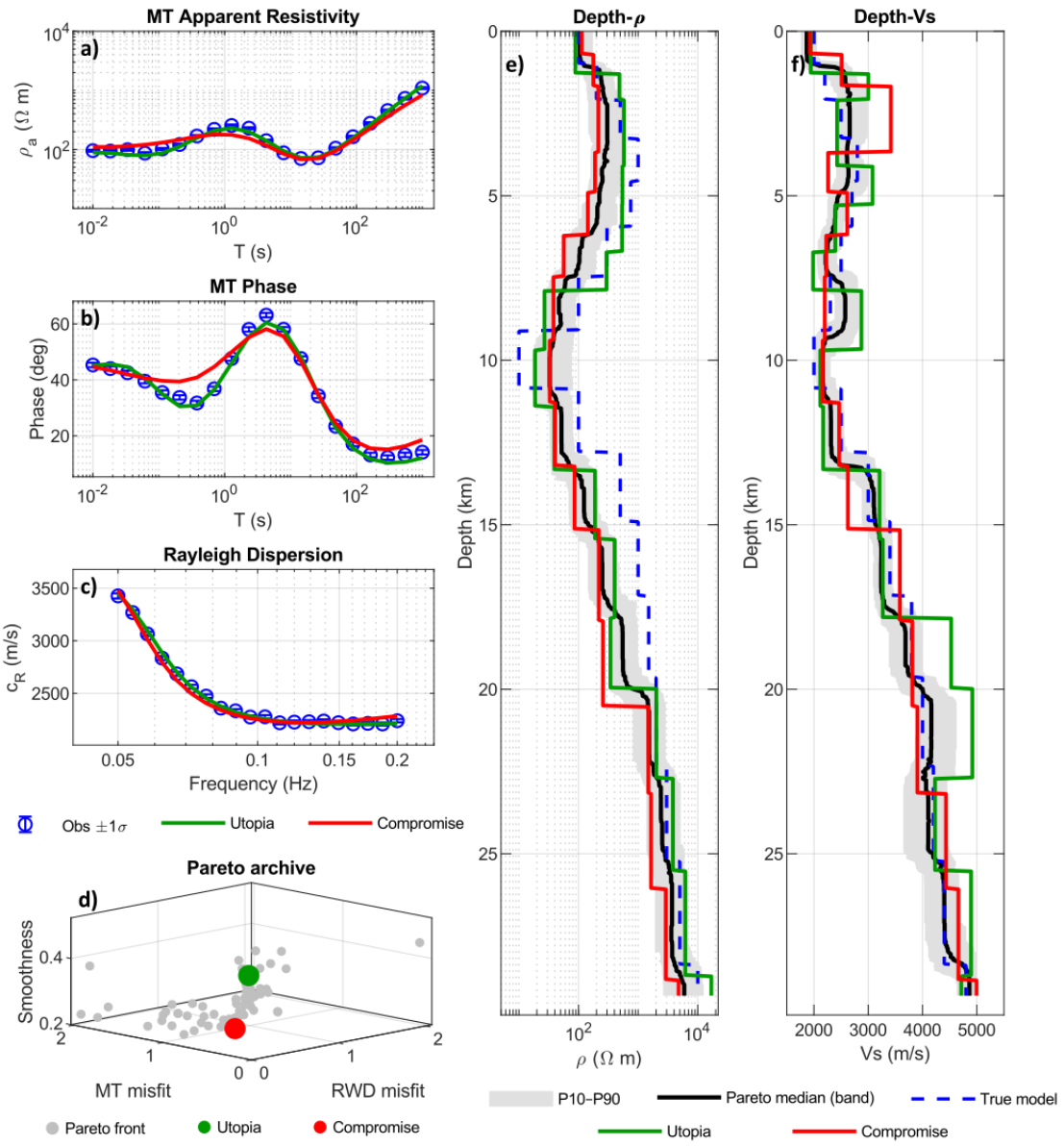

Figure S2. Results of noise-sensitivity example for the 5% noisy-coupled case. a) Apparent resistivity, b) Phase data and c) RWD fit with the predicted responses of the selected representative solutions. d) Three-objective Pareto, highlighting the utopia and compromise solutions. e) $\rho(z)$ and f) $V_s(z)$ models for the true model and the selected utopia and compromise solutions, together with the P10–P90 envelope and the Pareto-median profile from the repository.

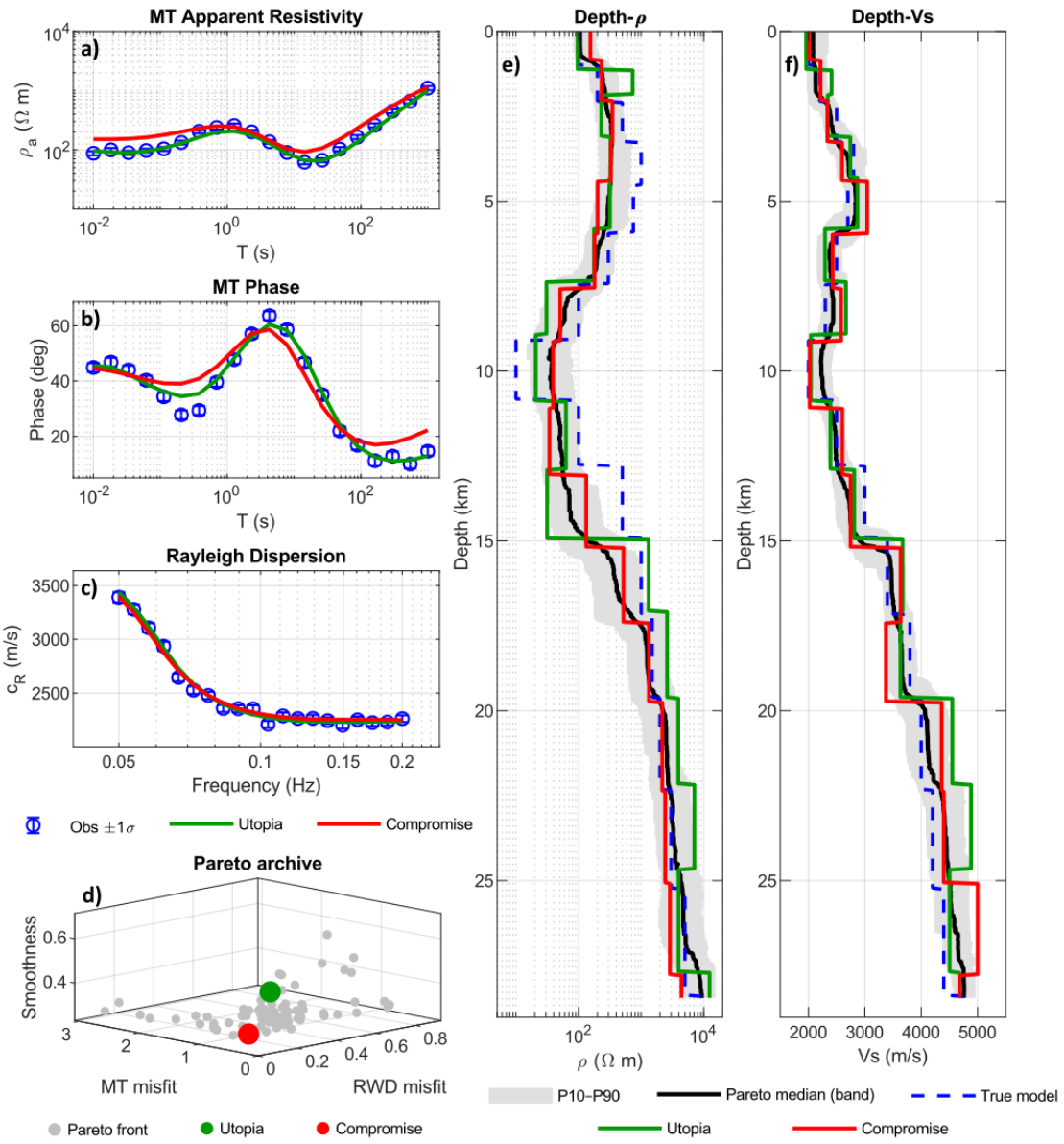

Figure S3. Results of noise-sensitivity example for the 10% noisy-coupled case. a) Apparent resistivity, b) Phase data and c) RWD fit with the predicted responses of the selected representative solutions. d) Three-objective Pareto, highlighting the utopia and compromise solutions. e) $\rho(z)$ and f) $V_s(z)$ models for the true model and the selected utopia and compromise solutions, together with the P10–P90 envelope and the Pareto-median profile from the repository.

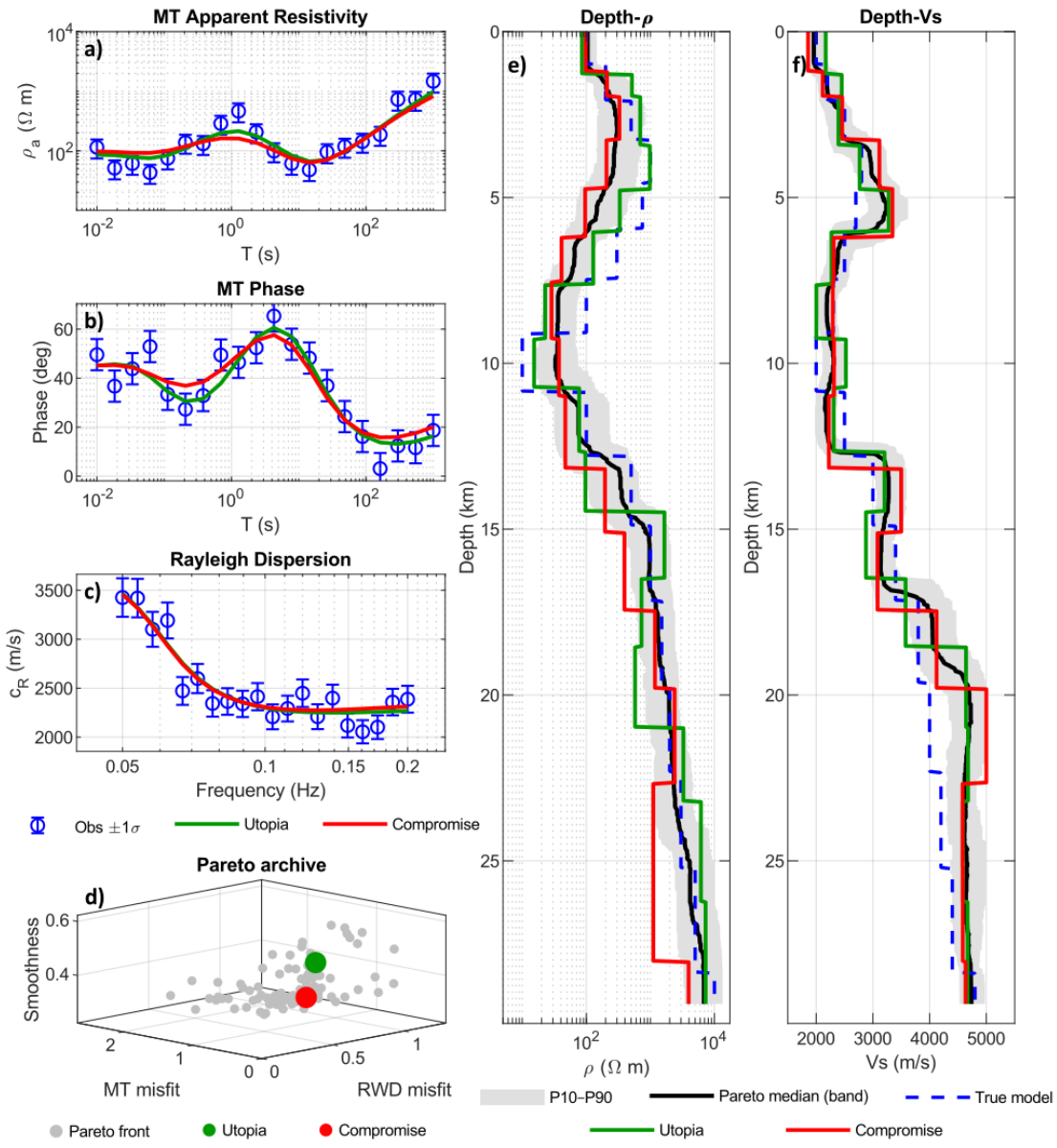

Figure S4. Results of noise-sensitivity example for the 40% noisy-coupled case. a) Apparent resistivity, b) Phase data and c) RWD fit with the predicted responses of the selected representative solutions. d) Three-objective Pareto, highlighting the utopia and compromise solutions. e) $\rho(z)$ and f) $V_s(z)$ models for the true model and the selected utopia and compromise solutions, together with the P10–P90 envelope and the Pareto-median profile from the repository.

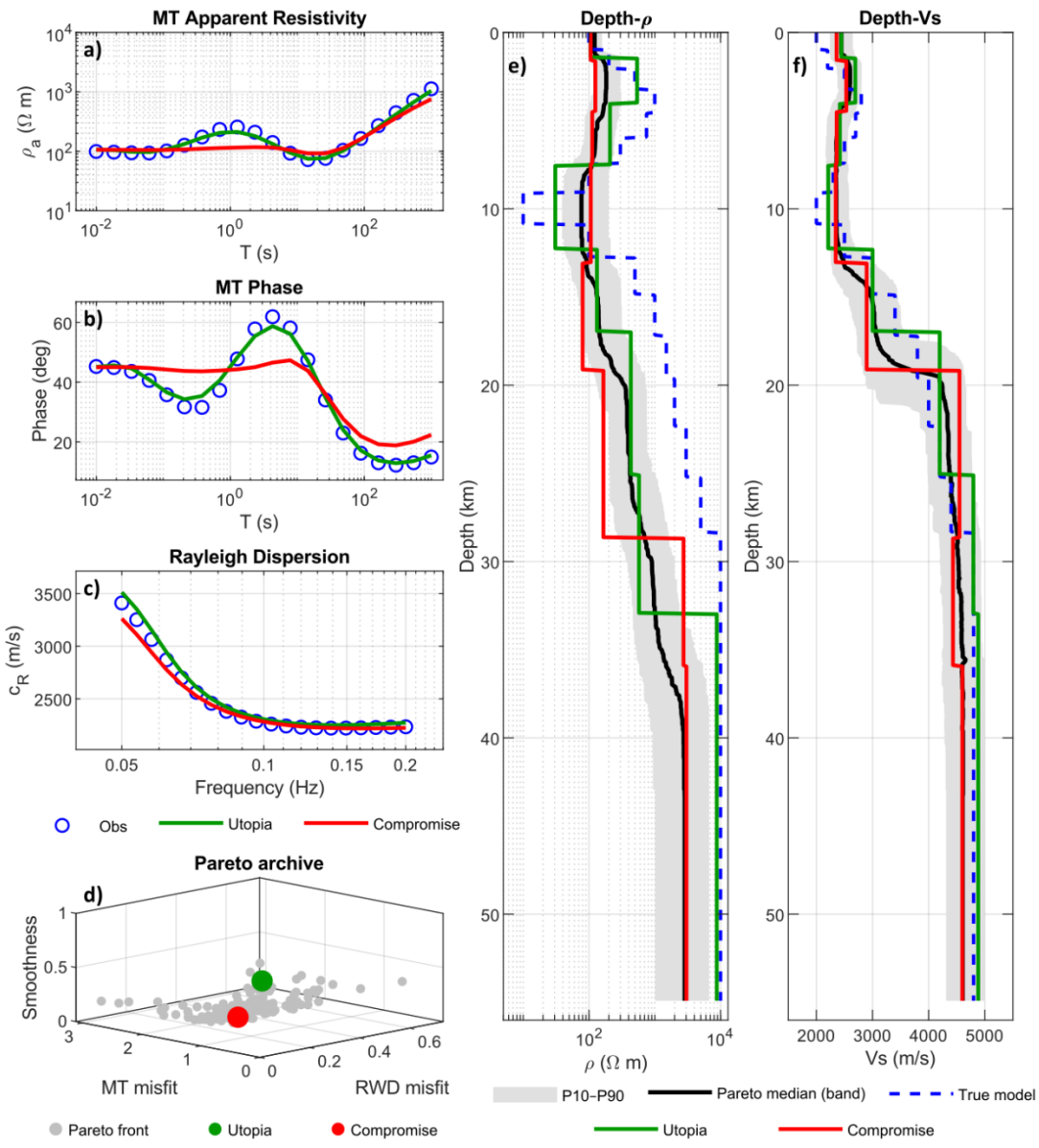

Figure S5. Results of layering-sensitivity example for the h=8 layers. a) Apparent resistivity, b) Phase data and c) RWD fit with the predicted responses of the selected representative solutions. d) Three-objective Pareto, highlighting the utopia and compromise solutions. e) $\rho(z)$ and f) $V_s(z)$ models for the true model and the selected utopia and compromise solutions, together with the P10–P90 envelope and the Pareto-median profile from the repository.

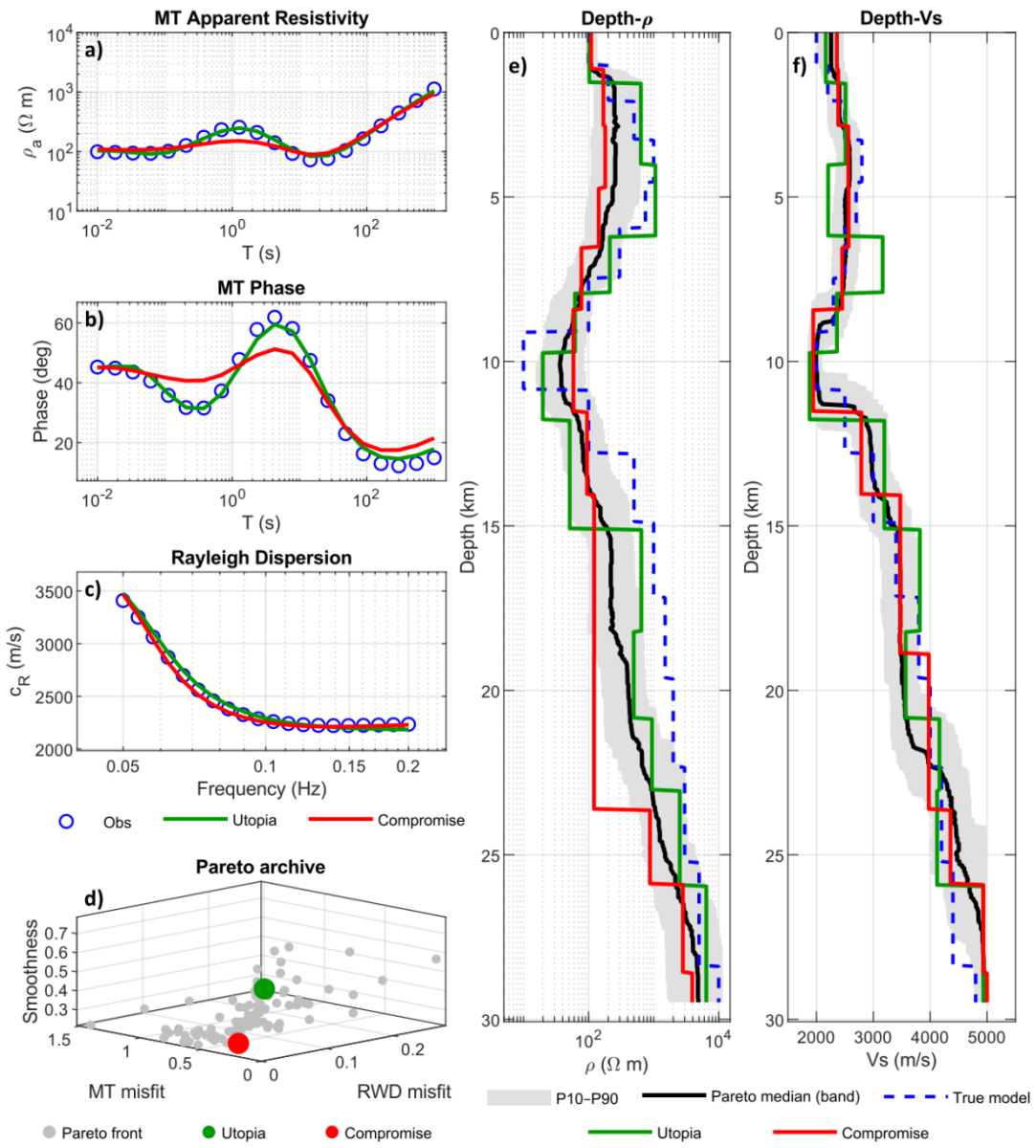

Figure S6. Results of layering-sensitivity example for the h=12 layers. a) Apparent resistivity, b) Phase data and c) RWD fit with the predicted responses of the selected representative solutions. d) Three-objective Pareto, highlighting the utopia and compromise solutions. e) $\rho(z)$ and f) $V_s(z)$ models for the true model and the selected utopia and compromise solutions, together with the P10–P90 envelope and the Pareto-median profile from the repository.

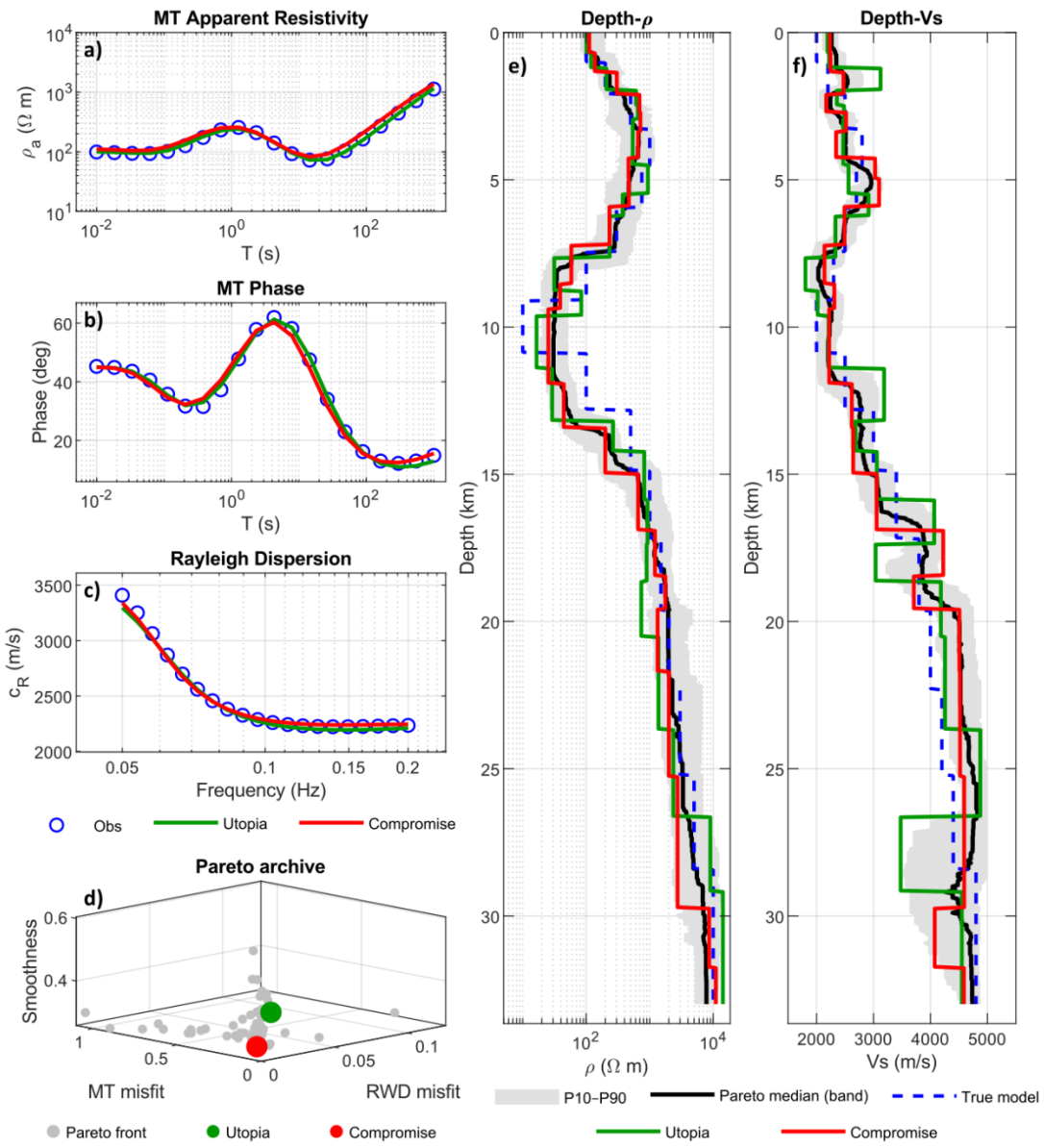

Figure S7. Results of layering-sensitivity example for the h=22 layers. a) Apparent resistivity, b) Phase data and c) RWD fit with the predicted responses of the selected representative solutions. d) Three-objective Pareto, highlighting the utopia and compromise solutions. e) $\rho(z)$ and f) $V_s(z)$ models for the true model and the selected utopia and compromise solutions, together with the P10–P90 envelope and the Pareto-median profile from the repository.

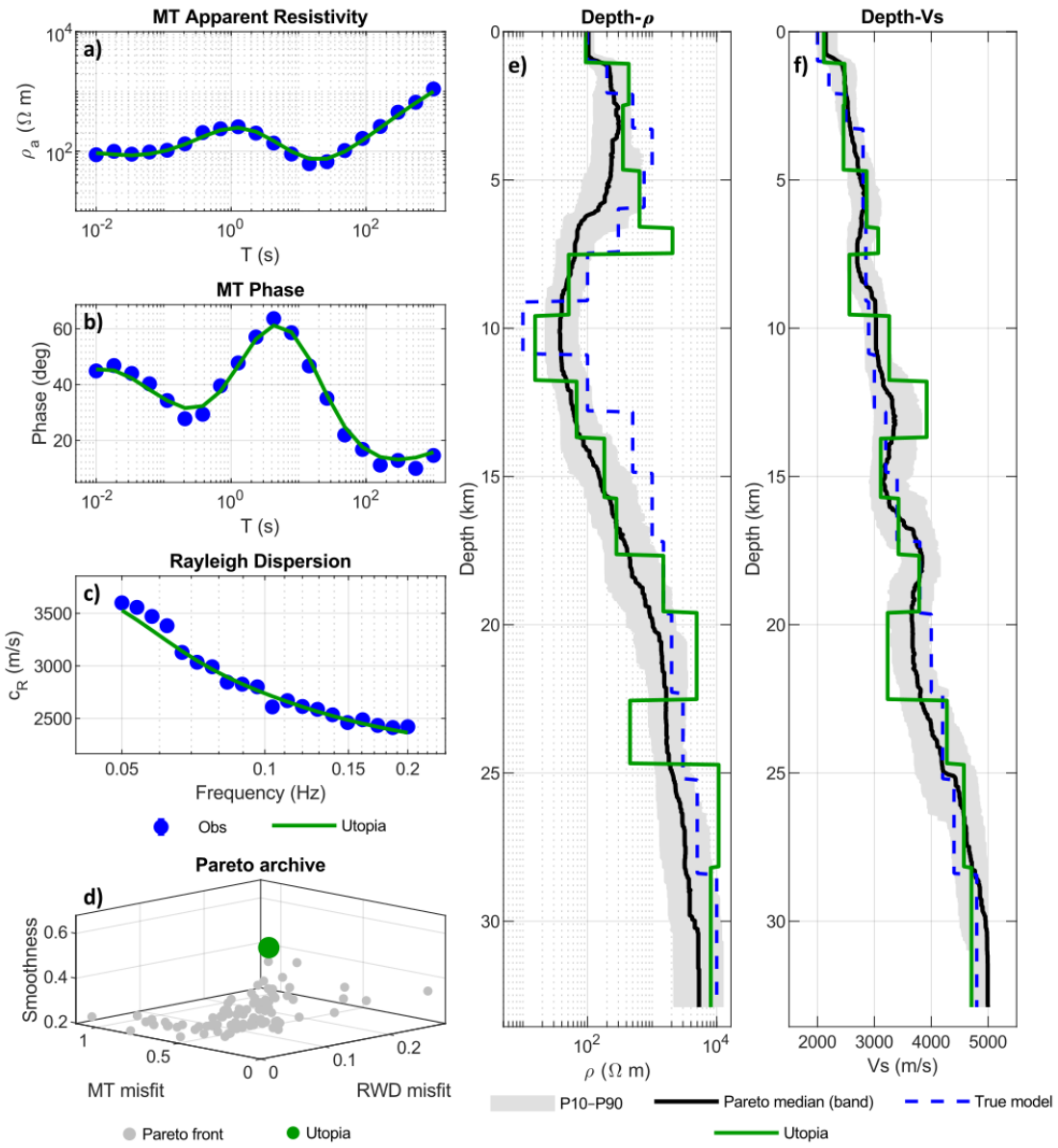

Figure S8. Results of noise-sensitivity example for the 10% noisy-decoupled case#1. a) Apparent resistivity, b) Phase data and c) RWD fit with the predicted responses of the utopia solution. d) Three-objective Pareto archive, highlighting the utopia solution. e) $\rho(z)$ and f) $V_s(z)$ for the true model and the selected utopia solution, together with the P10–P90 envelope and the Pareto-median profile from the repository.

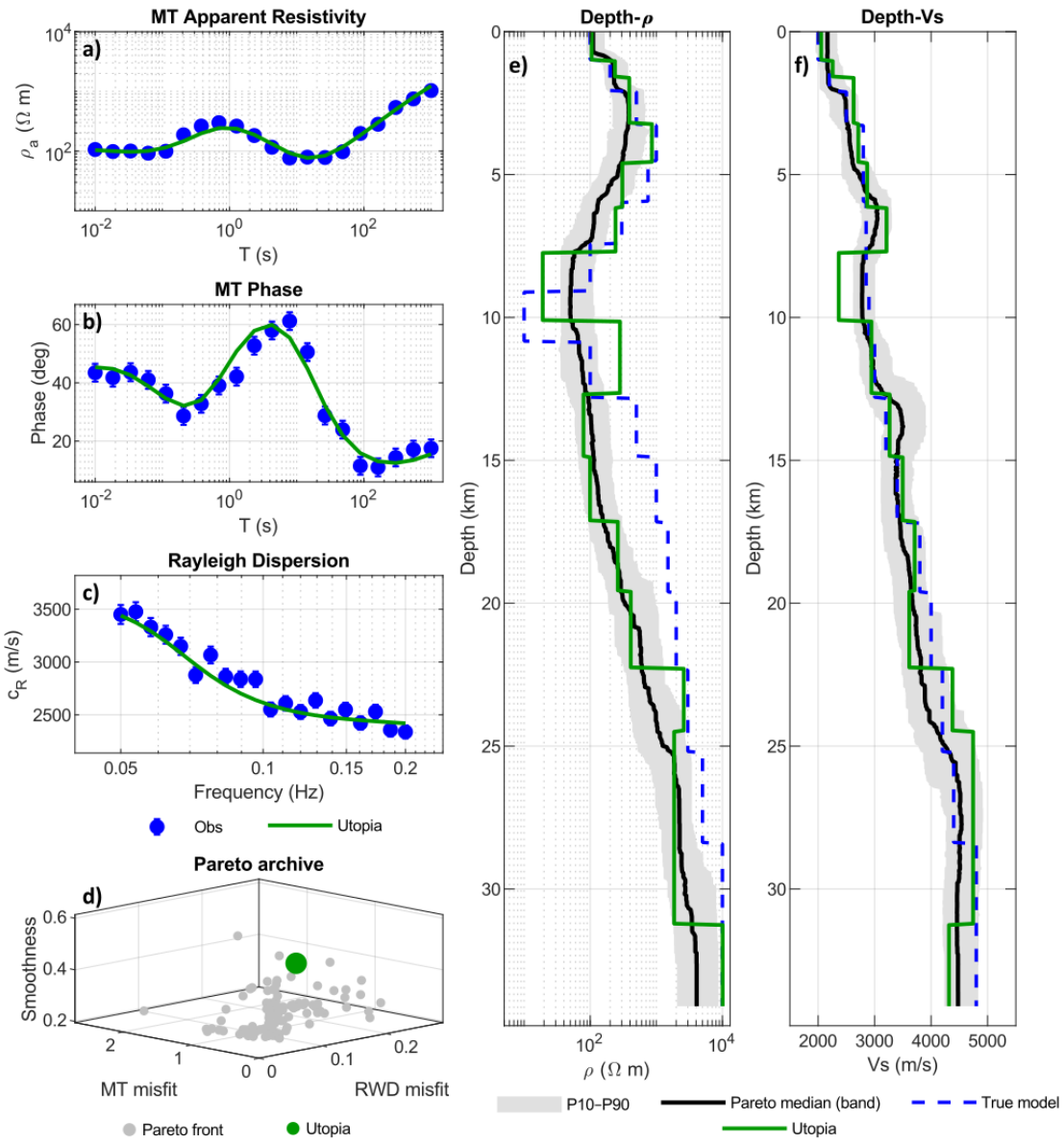

Figure S9. Results of noise-sensitivity example for the 20% noisy-decoupled case#1. a) Apparent resistivity, b) Phase data and c) RWD fit with the predicted responses of the utopia solution. d) Three-objective Pareto archive, highlighting the utopia solution. e) $\rho(z)$ and f) $V_s(z)$ for the true model and the selected utopia solution, together with the P10–P90 envelope and the Pareto-median profile from the repository.

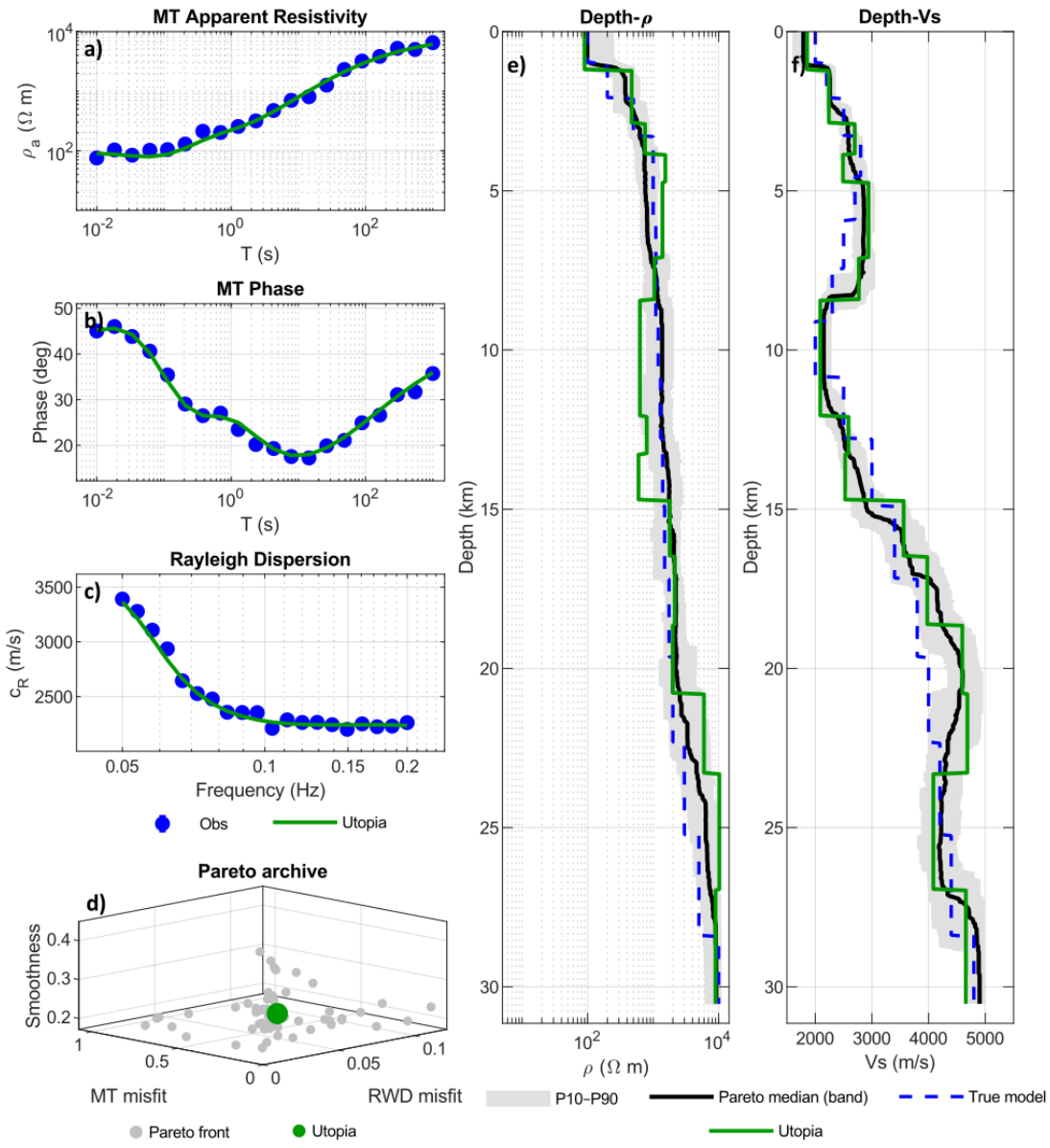

Figure S10. Results of noise-sensitivity example for the 10% noisy-decoupled case#2. a) Apparent resistivity, b) Phase data and c) RWD fit with the predicted responses of the utopia solution. d) Three-objective Pareto archive, highlighting the utopia solution. e) $\rho(z)$ and f) $V_s(z)$ for the true model and the selected utopia solution, together with the P10–P90 envelope and the Pareto-median profile from the repository.

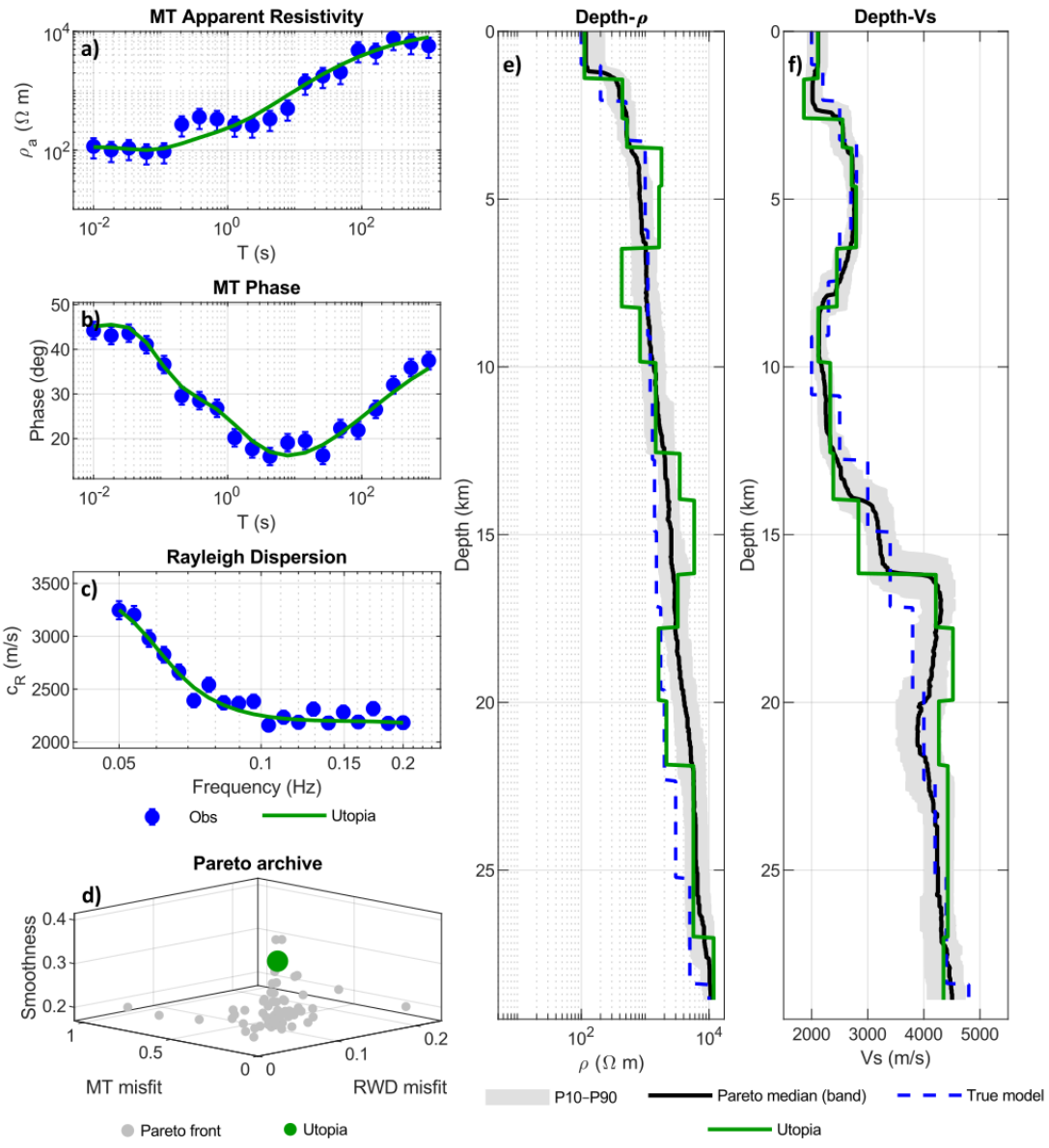

Figure S11. Results of noise-sensitivity example for the 20% noisy-decoupled case#2. a) Apparent resistivity, b) Phase data and c) RWD fit with the predicted responses of the utopia solution. d) Three-objective Pareto archive, highlighting the utopia solution. e) $\rho(z)$ and f) $V_s(z)$ for the true model and the selected utopia solution, together with the P10–P90 envelope and the Pareto-median profile from the repository.

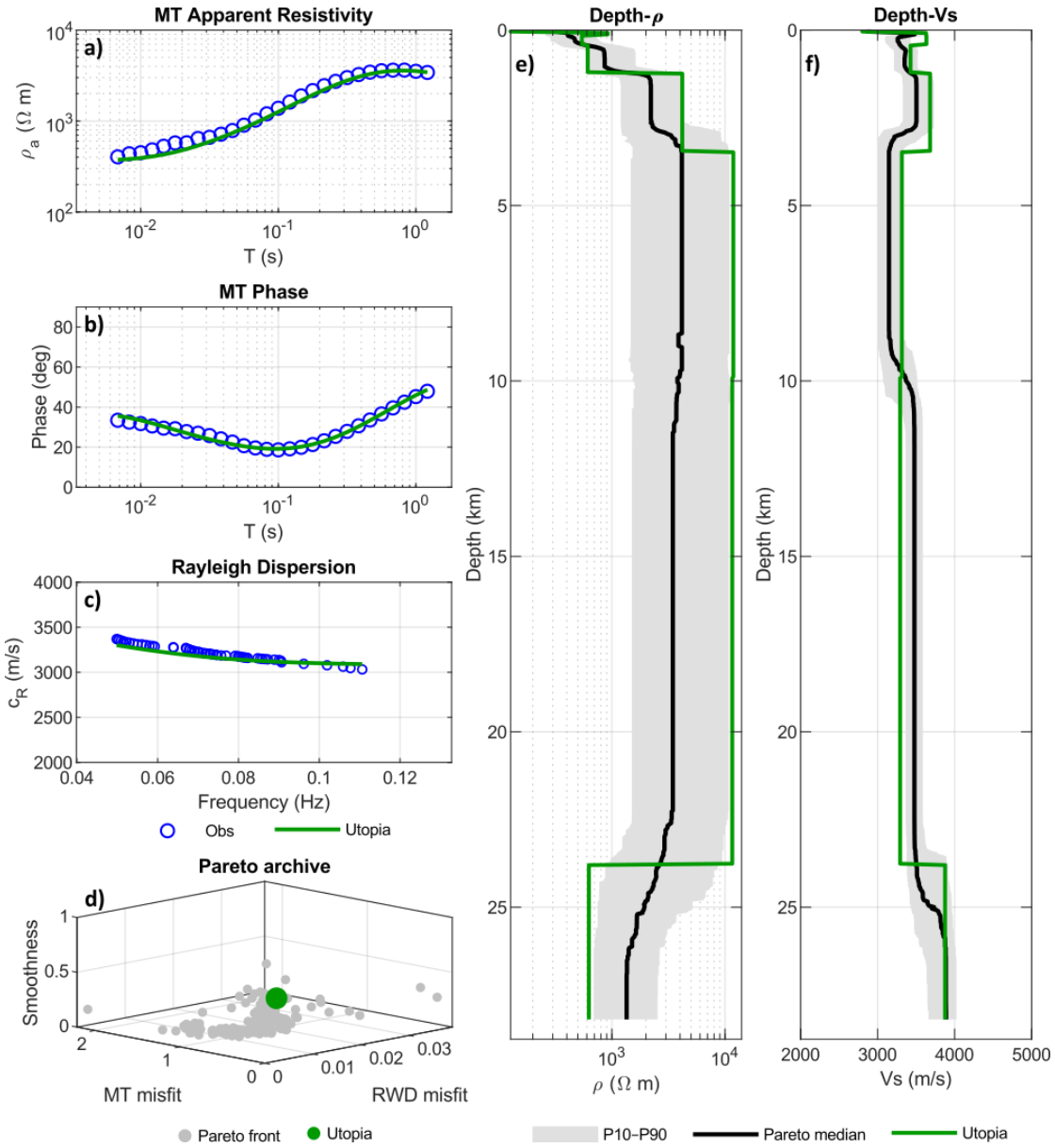

Figure S12. Results of the KEp for h =8 layers. a) Apparent resistivity, b) Phase data and c) RWD fit with the predicted responses of the utopia solution. d) Three-objective Pareto archive, highlighting the utopia solution. e) $\rho(z)$ and f) $V_s(z)$ models for the selected utopia solution, together with the P10–P90 envelope and the Pareto-median profile from the repository.

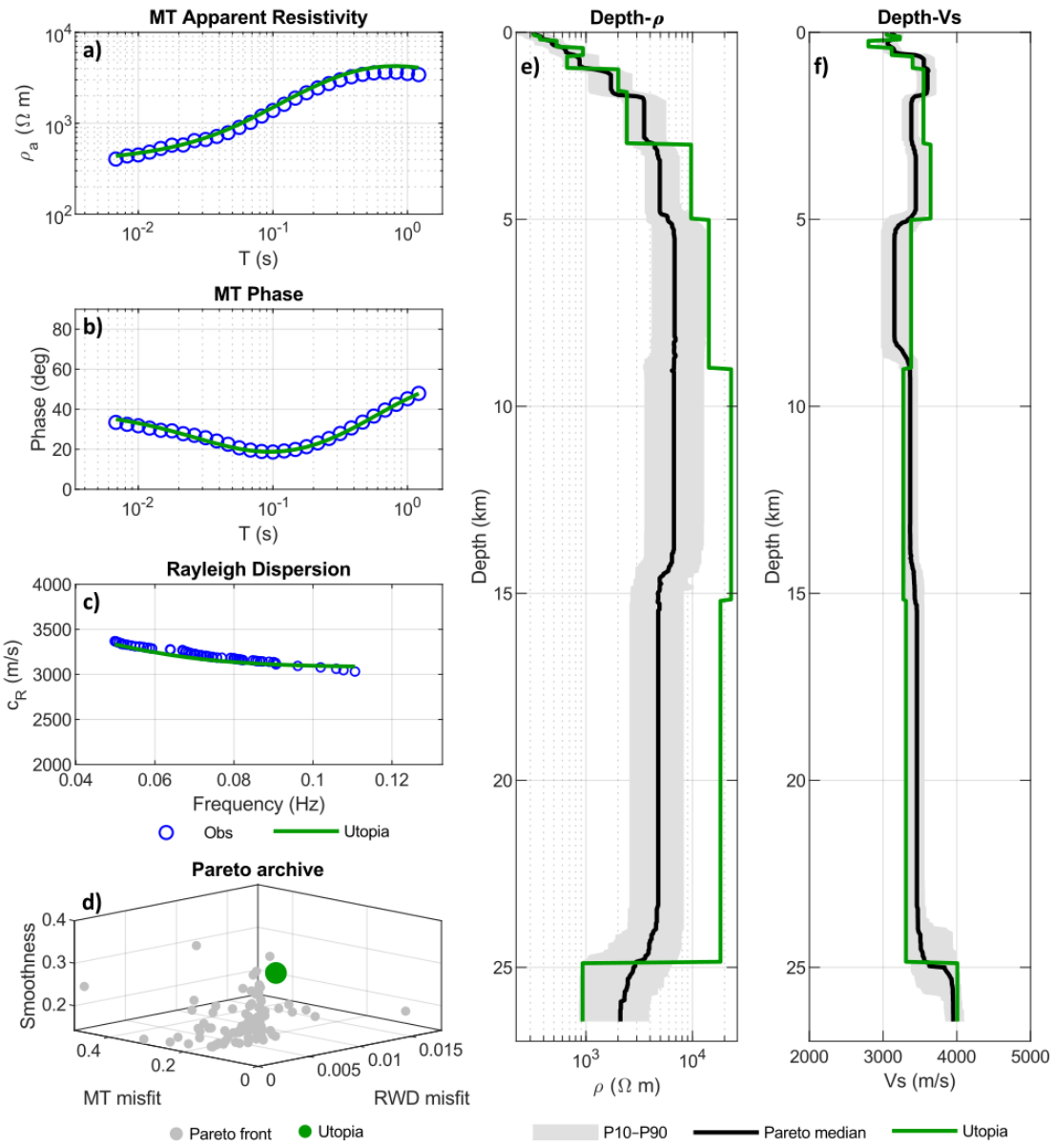

Figure S13. Results of the KEp for h =12 layers. a) Apparent resistivity, b) Phase data and c) RWD fit with the predicted responses of the utopia solution. d) Three-objective Pareto archive, highlighting the utopia solution. e) $\rho(z)$ and f) $V_s(z)$ models for the selected utopia solution, together with the P10–P90 envelope and the Pareto-median profile from the repository.

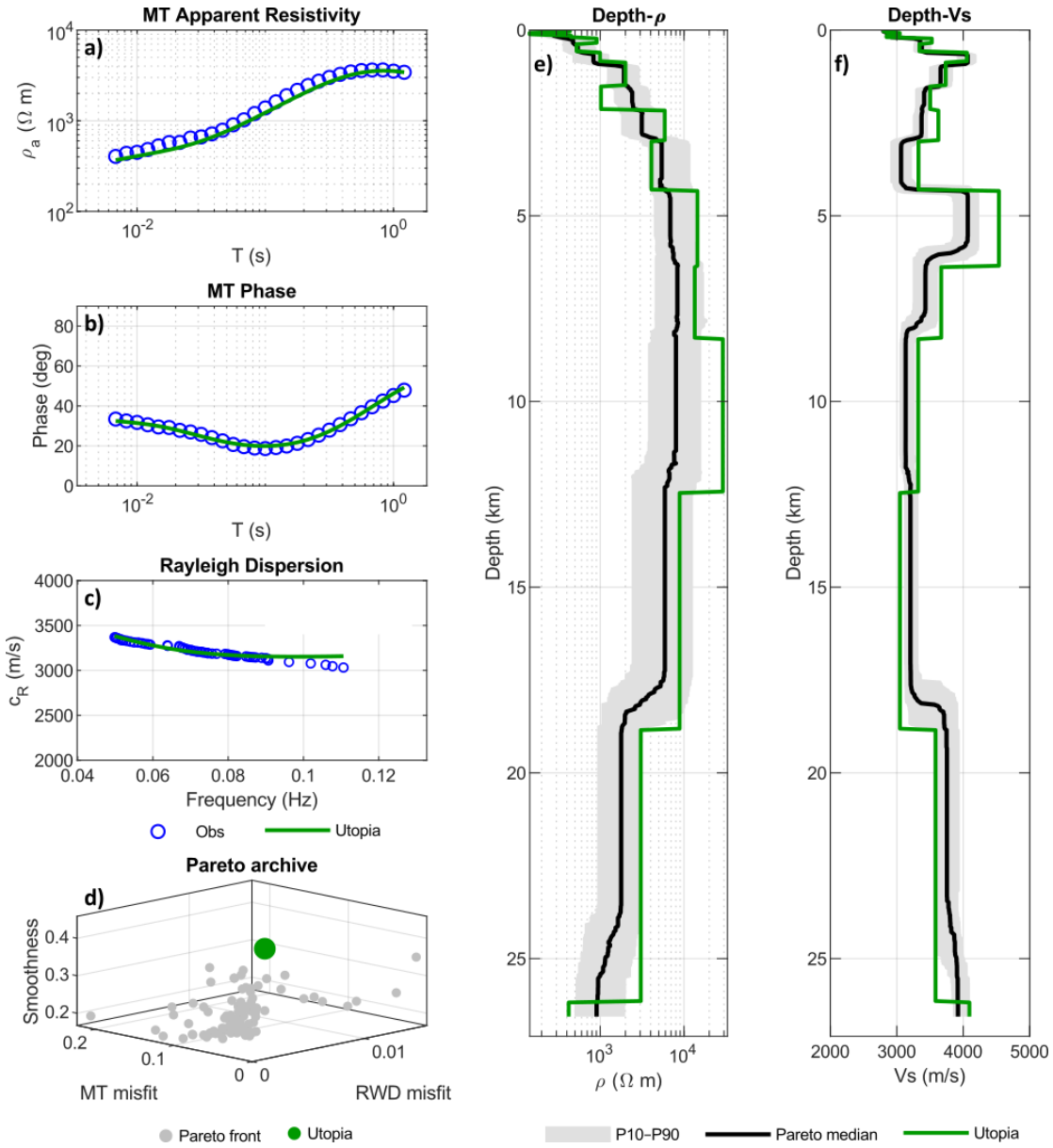

Figure S14. Results of the KEp for h =16 layers. a) Apparent resistivity, b) Phase data and c) RWD fit with the predicted responses of the utopia solution. d) Three-objective Pareto archive, highlighting the utopia solution. e) $\rho(z)$ and f) $V_s(z)$ models for the selected utopia solution, together with the P10–P90 envelope and the Pareto-median profile from the repository.

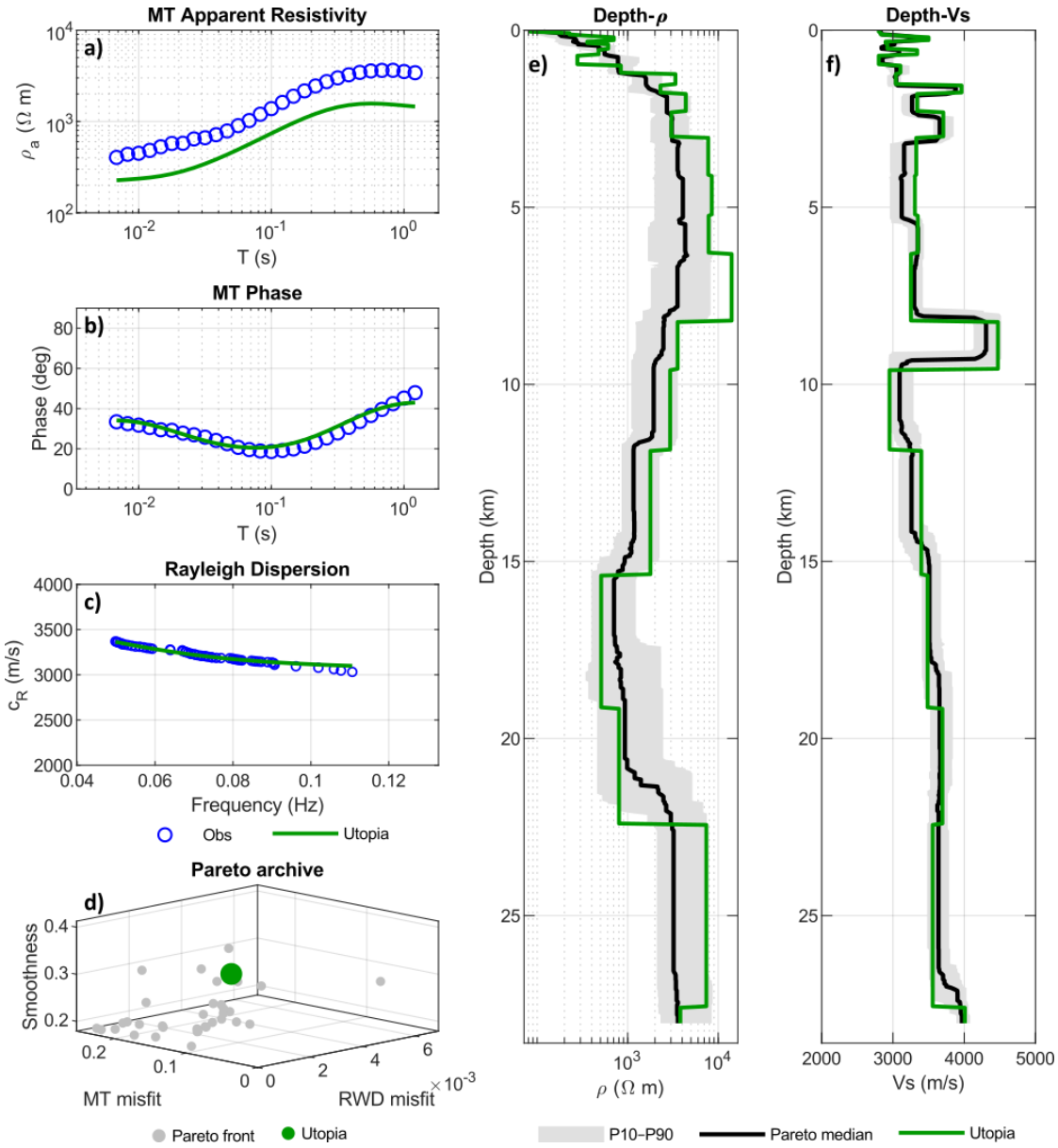

Figure S15. Results of the KEp for h =24 layers. a) Apparent resistivity, b) Phase data and c) RWD fit with the predicted responses of the utopia solution. d) Three-objective Pareto archive, highlighting the utopia solution. e) $\rho(z)$ and f) $V_s(z)$ models for the selected utopia solution, together with the P10–P90 envelope and the Pareto-median profile from the repository.

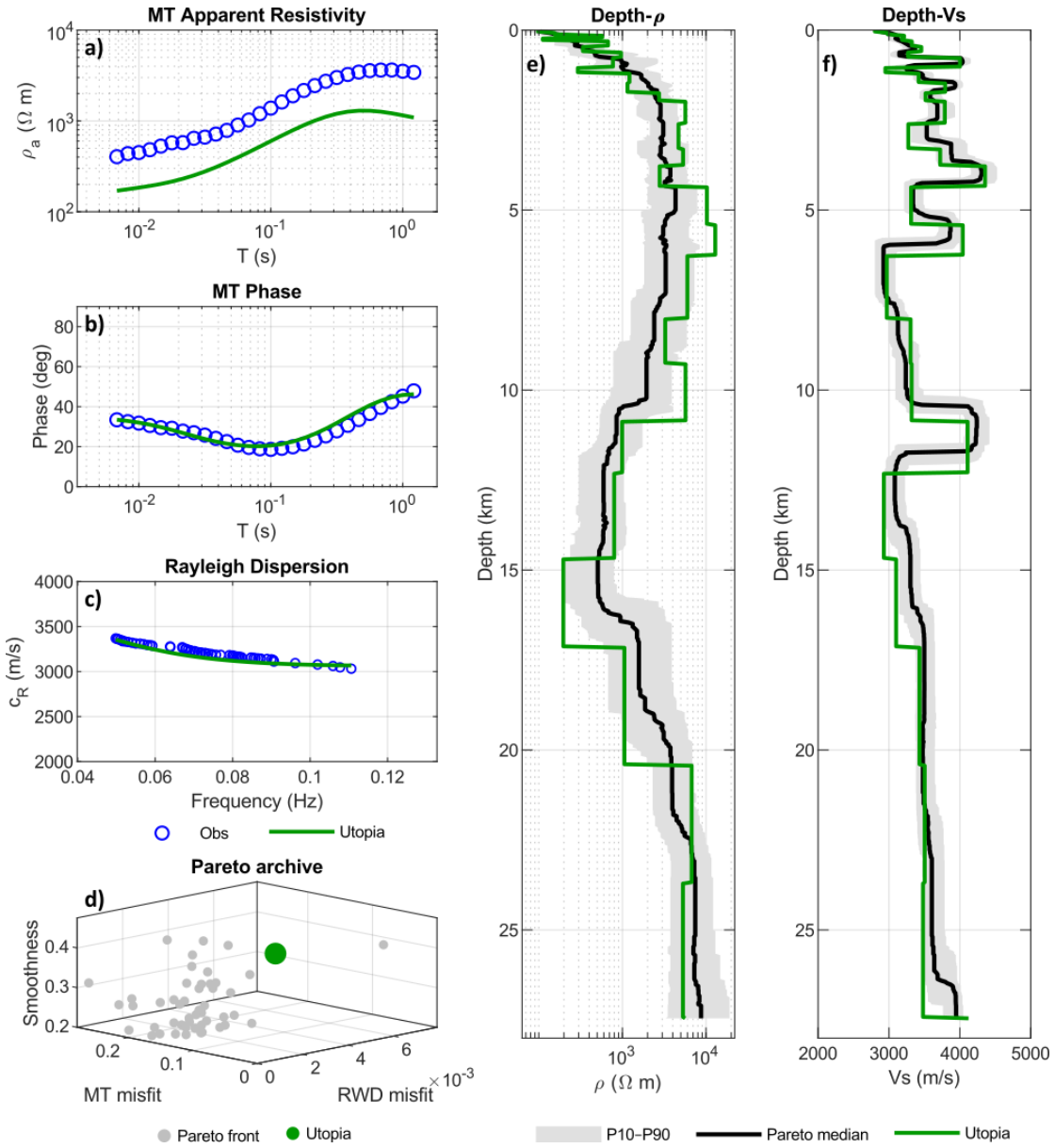

Figure S16. Results of the KEp for h =28 layers. a) Apparent resistivity, b) Phase data and c) RWD fit with the predicted responses of the utopia solution. d) Three-objective Pareto archive, highlighting the utopia solution. e) $\rho(z)$ and f) $V_s(z)$ models for the selected utopia solution, together with the P10–P90 envelope and the Pareto-median profile from the repository.

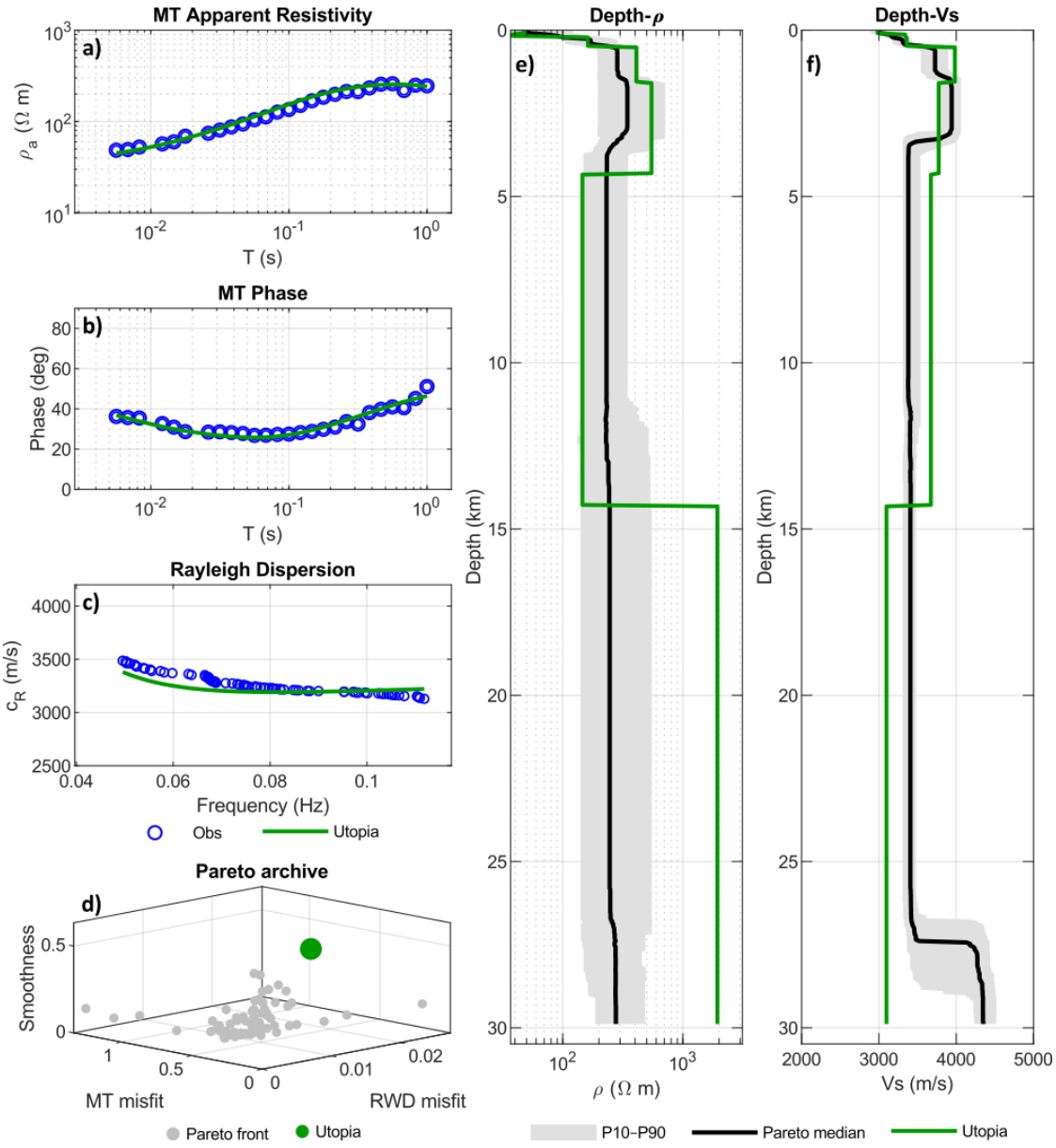

Figure S17. Results of the GBp for h =8 layers. a) Apparent resistivity, b) Phase data and c) RWD fit with the predicted responses of the utopia solution. d) Three-objective Pareto archive, highlighting the utopia solution. e) $\rho(z)$ and f) $V_s(z)$ models for the selected utopia solution, together with the P10–P90 envelope and the Pareto-median profile from the repository.

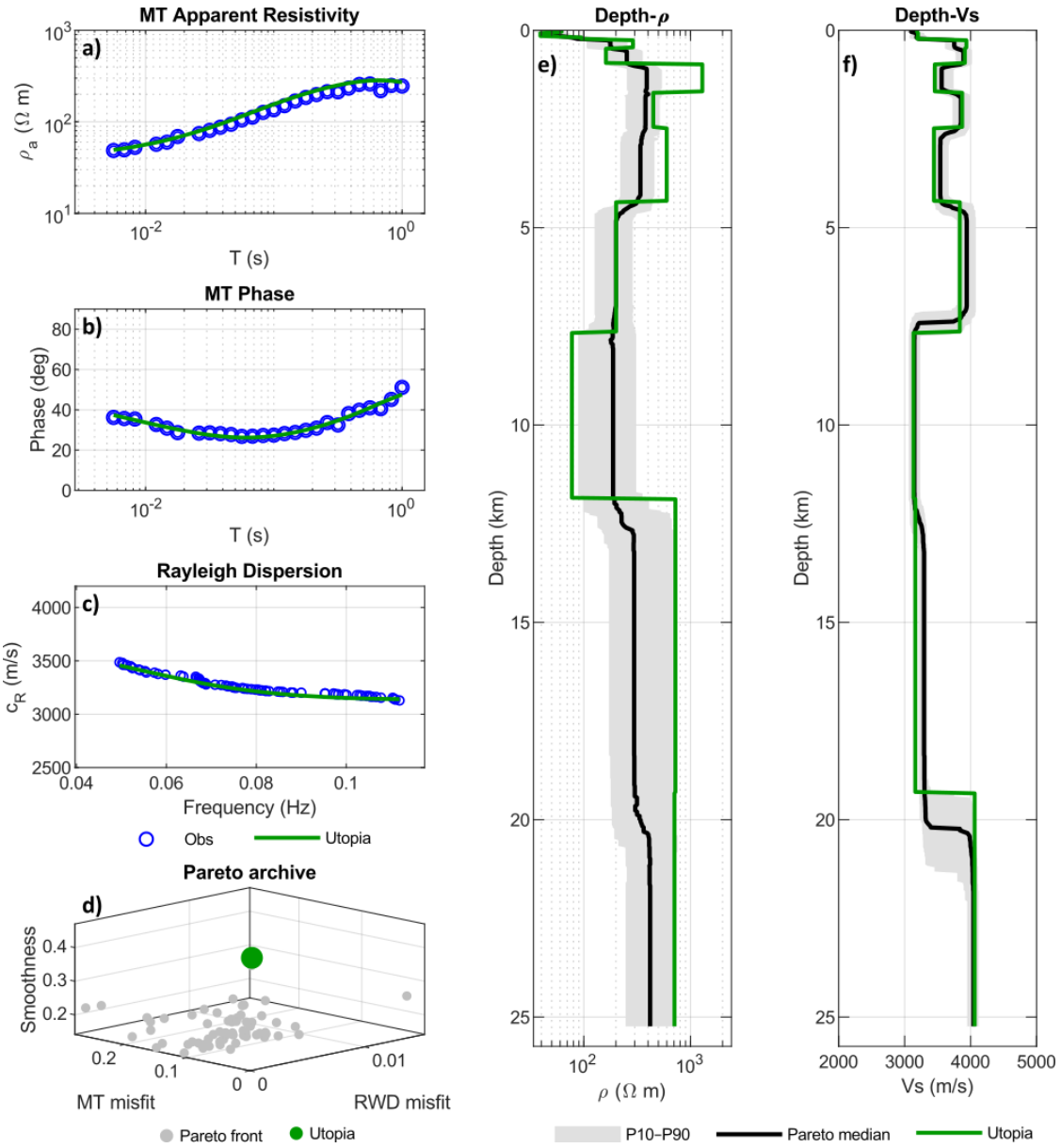

Figure S18. Results of the GBp for h =12 layers. a) Apparent resistivity, b) Phase data and c) RWD fit with the predicted responses of the utopia solution. d) Three-objective Pareto archive, highlighting the utopia solution. e) $\rho(z)$ and f) $V_s(z)$ models for the selected utopia solution, together with the P10–P90 envelope and the Pareto-median profile from the repository.

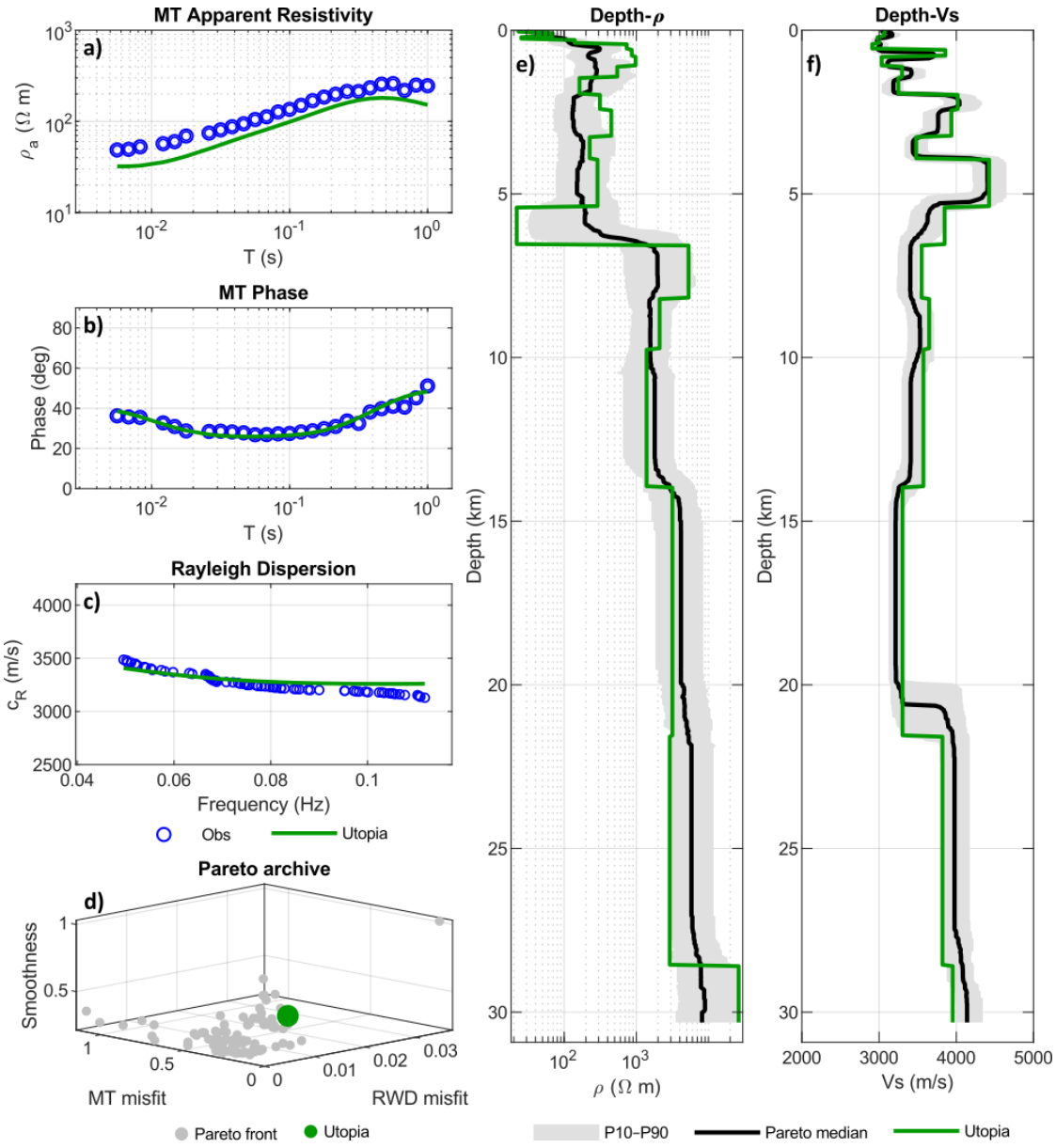

Figure S19. Results of the GBp for h =20 layers. a) Apparent resistivity, b) Phase data and c) RWD fit with the predicted responses of the utopia solution. d) Three-objective Pareto archive, highlighting the utopia solution. e) $\rho(z)$ and f) $V_s(z)$ models for the selected utopia solution, together with the P10–P90 envelope and the Pareto-median profile from the repository.

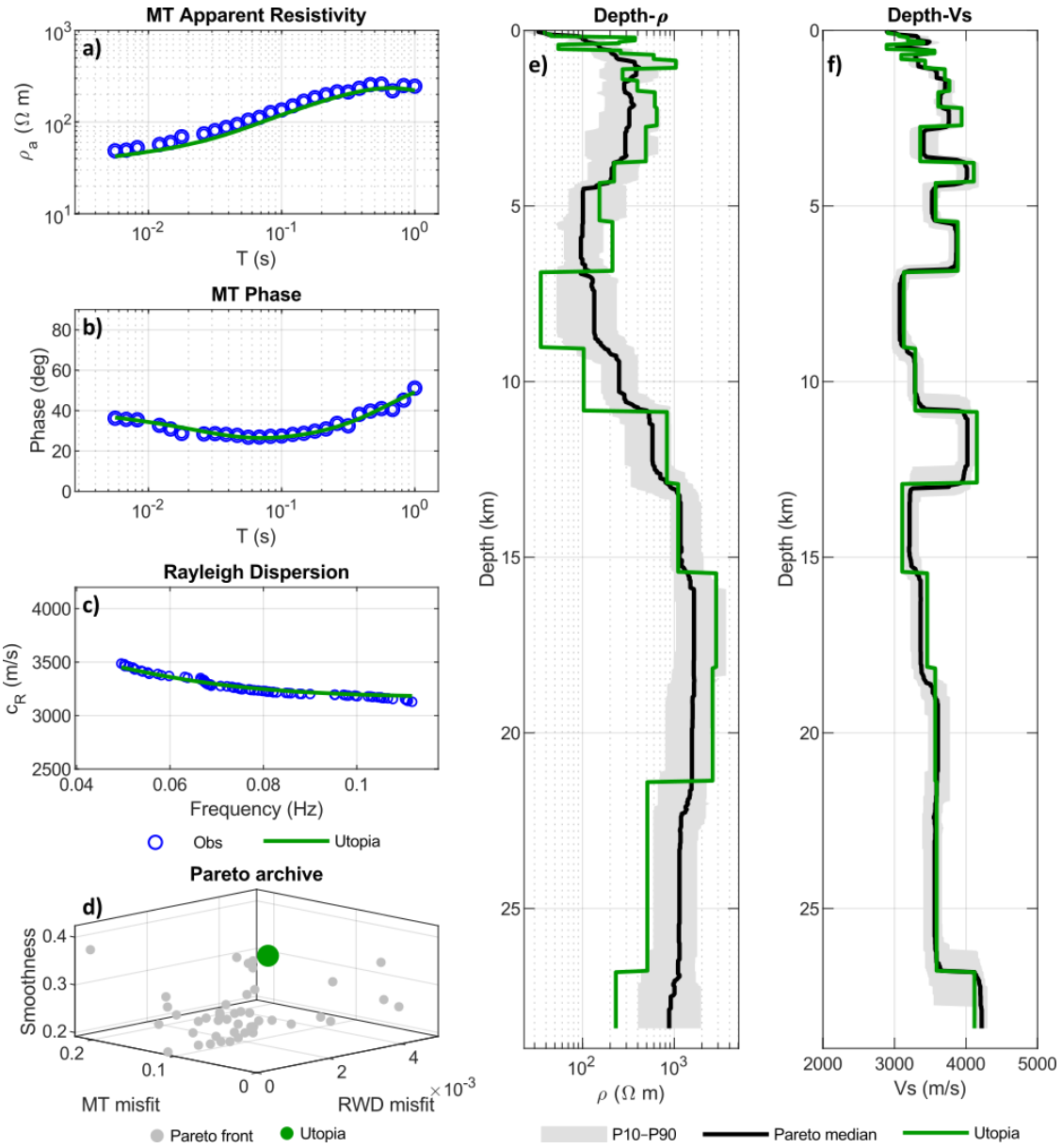

Figure S20. Results of the GBp for h =24 layers. a) Apparent resistivity, b) Phase data and c) RWD fit with the predicted responses of the utopia solution. d) Three-objective Pareto archive, highlighting the utopia solution. e) $\rho(z)$ and f) $V_s(z)$ models for the selected utopia solution, together with the P10–P90 envelope and the Pareto-median profile from the repository.

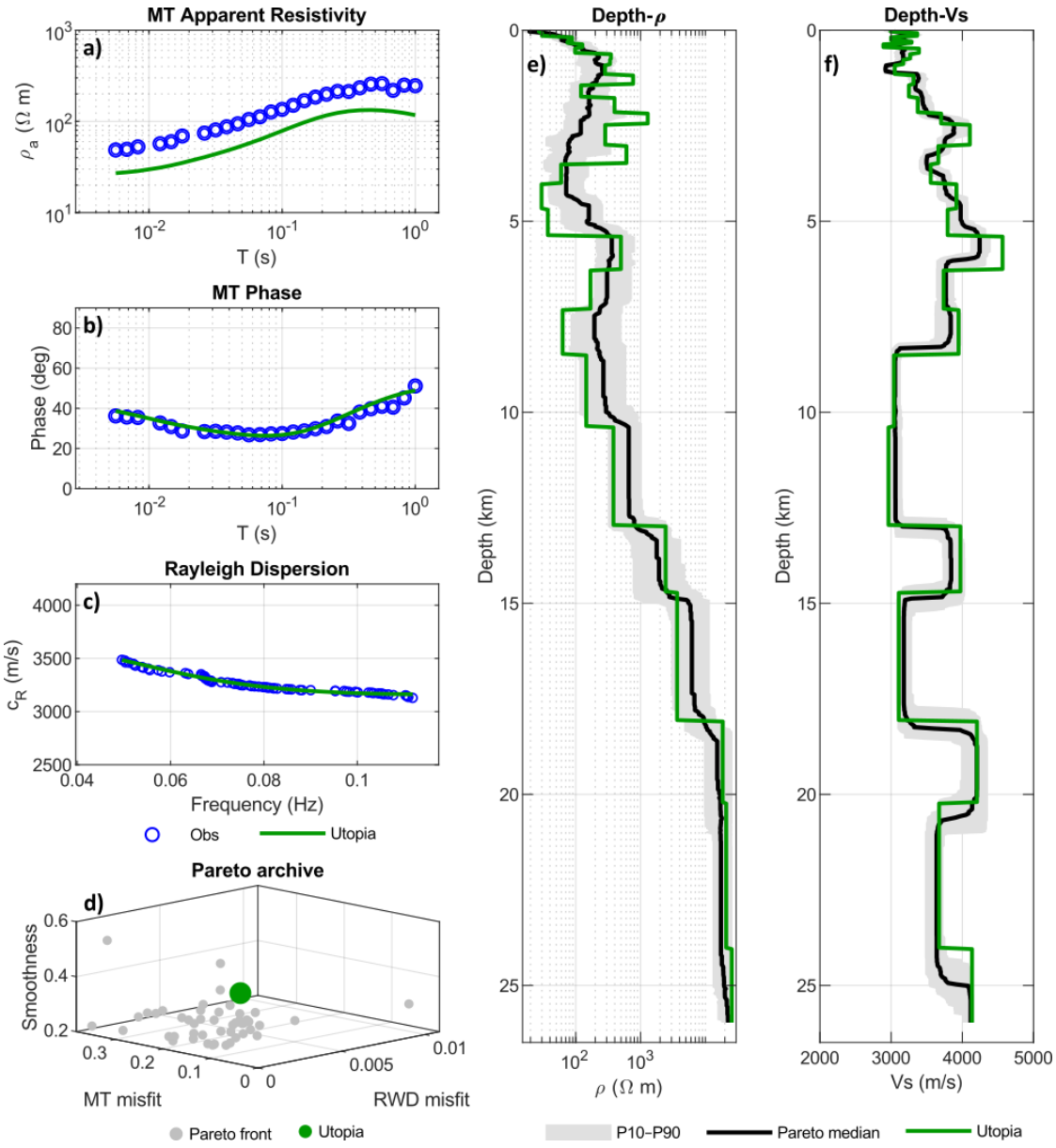

Figure S21. Results of the GBp for h =28 layers. a) Apparent resistivity, b) Phase data and c) RWD fit with the predicted responses of the utopia solution. d) Three-objective Pareto archive, highlighting the utopia solution. e) $\rho(z)$ and f) $V_s(z)$ models for the selected utopia solution, together with the P10–P90 envelope and the Pareto-median profile from the repository.